Radiation Shielding of Heavy Ion Beam Focussing Magnets in HIBALL

M.E. Sawan, W.F. Vogelsang, and D.K. Sze

August 1981

UWFDM-438

Trans. ANS 39 (1981) 777.

FUSION TECHNOLOGY INSTITUTE

UNIVERSITY OF WISCONSIN

MADISON WISCONSIN

Radiation Shielding of Heavy Ion Beam Focussing Magnets in HIBALL

M.E. Sawan, W.F. Vogelsang, and D.K. Sze

Fusion Technology Institute
University of Wisconsin
1500 Engineering Drive
Madison, WI 53706

http://fti.neep.wisc.edu

August 1981

UWFDM-438

Trans. ANS 39 (1981) 777.

Radiation Shielding of Heavy Ion Beam Focussing Magnets in HIBALL

M.E. Sawan

W.F. Vogelsang

D.K. Sze

August 1981

UWFDM-438

I. Introduction

Fusion reactors are required to accommodate a variety of penetrations. The purpose and size of these penetrations vary depending on the reactor type.[1-3] Proper shielding is required to protect the vital components in the penetration from excessive radiation damage caused by radiation streaming. A major penetration in a heavy ion beam fusion reactor is the ion beam line penetration. Such a penetration is characterized by a large size. Furthermore, a large number of these penetrations is required to provide uniform illumination of the target.

The HIBALL reactor utilizes twenty 10 GeV Bi^{++} ion beams to bring the target to ignition. Each beam port is rectangular in shape with a height of 102.8 and a width of 34.3 cm at the reactor cavity wall of radius 7 m. There will be 8.14×10^{16} neutrons streaming through each beam line penetration per shot for a DT yield of 400 MJ. A number of superconducting magnets are arranged along the beam line to focus the ion beam to a spot 6 mm in diameter at the target. Adequate penetration shielding is required to protect these beam focussing magnets from excessive radiation damage.

Various beam line penetration shield shapes have been considered to assess their effectiveness in reducing the radiation effects in the HIBALL beam focussing magnets. A three-dimensional neutronics and photonics analysis must be performed to account for the geometrical complexity of the penetration. The design criteria used to determine the shielding requirements for the magnets are:

1) A 50% radiation induced resistivity increase in the copper stabilizer which corresponds to 1.4×10^{-4} dpa (displacements per atom).

2) A radiation dose of 5×10^{9} Rad in the epoxy electrical insulation.

3) A peak nuclear heating of 10^{-4} W/cm^3 in the magnet.

II. Calculational Model

The blanket region in HIBALL is 2 m thick and consists of SiC tubes through which $Li_{17}Pb_{83}$ liquid metal eutectic flows. The tubes occupy 33% of the blanket region. A cylindrical vacuum wall having a radius of 7 m is used. The first wall is made of ferritic steel (HT-9) and is 1 cm thick. A .4 m thick reflector composed of 90 v/o ferritic steel structure and 10 v/o $Li_{17}Pb_{83}$ coolant is used. The reactor utilizes a 3.5 m thick concrete biological shield. Because of its small thickness and negligible effect on radiation damage in the penetration, the first wall is neglected in the present analysis. The results presented here are based on a DT yield of 400 MJ and a repetition rate of 5 Hz yielding 7.1×10^{20} fusion neutrons per second. Neutron multiplication, spectrum softening and gamma production in the target have been taken into account by performing one-dimensional neutronics and photonics calculations[4] in the spherical target using the discrete ordinates code ANISN.[5]

The final focussing system in HIBALL which focusses the beam from the periodic beam line onto the target, consists of eight quadrupole magnets. The total length of the system is 60.4 m. Each quadrupole has a length of 2.7 m with the drift sections between the quadrupoles being 1.8 m long. Fig. 1 shows the vertical and horizontal envelopes for the beam as it is transported from the periodic line to the target. The positions of the eight quadrupoles used for focussing the beam are also shown. The inner dimensions of the magnet shield have been chosen to be at least 2 cm larger than the beam size, determined by the envelopes in Fig. 2, at all places along the penetration.

The 20 beam ports are arranged in two rows which are symmetric about the reactor midplane (z=0). The beam ports are 4 m apart vertically at the reactor vacuum wall. Because of symmetry only half a penetration is modelled

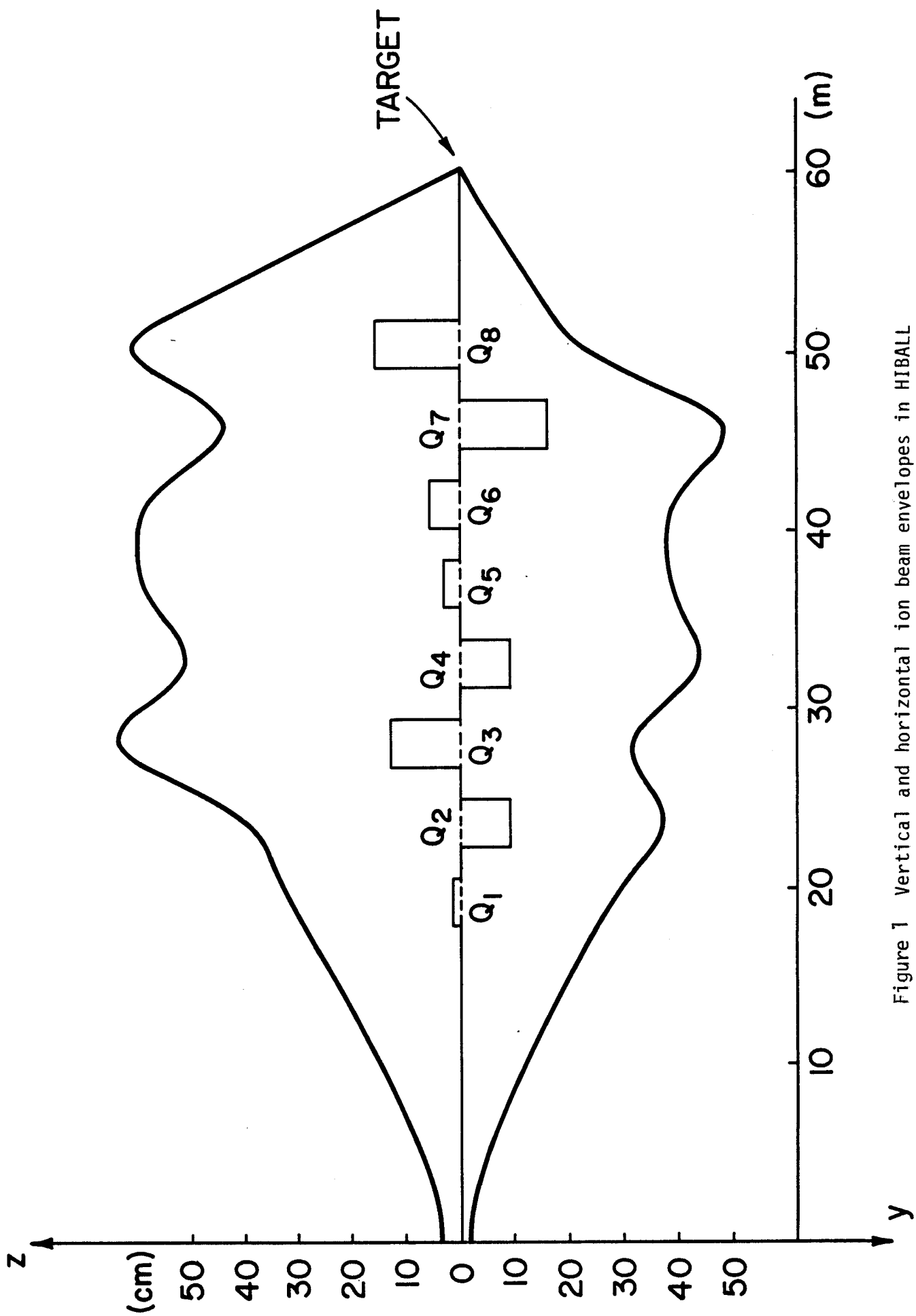

Figure 1 Vertical and horizontal ion beam envelopes in HIBALL

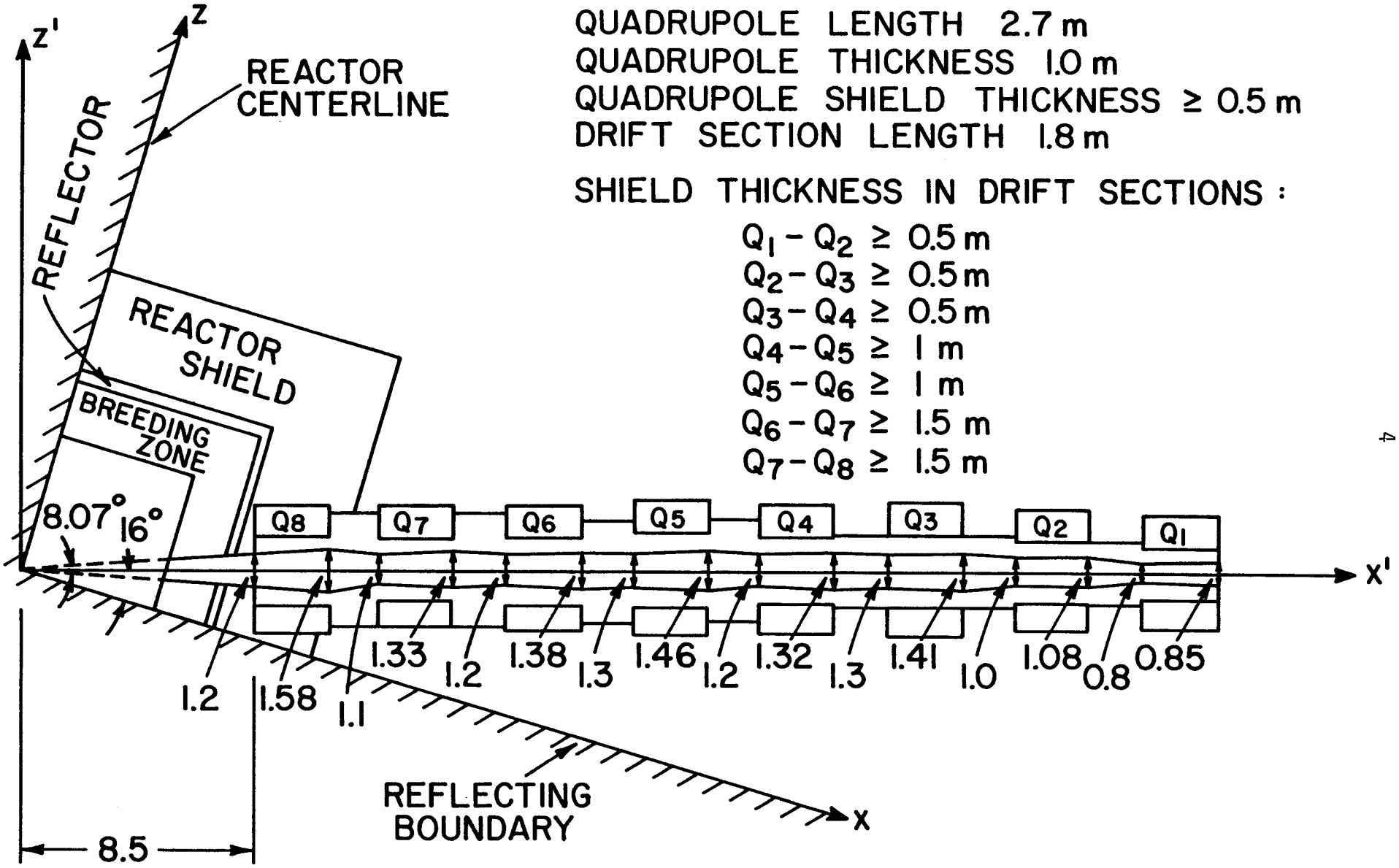

Figure 2 Vertical cross section for focussing magnets and shield

in the present analysis with reflecting albedo boundaries used at the planes of symmetry. Consequently, only 1/40 of the reactor is modelled. This corresponds to a "pie slice" of the upper half of the reactor with an azimuthal angle of 18°. The angle between the centerline of the beam line penetration and the reactor midplane is 16°. The axes are rotated by 16° around the y axis for the penetration centerline to coincide with the x axis of the calculational model. This simplifies the description of the penetration geometry. Fig. 2 gives the vertical cross section for the focussing magnets and shield. Fig. 3 gives the cross section at the plane z'=0. Each quadrupole has a length of 2.7 m and a thickness of 1 m. Each magnet coil is modelled as having 7.52 v/o NbTi superconductor coils, 67.48 v/o copper stabilizer, 15 v/o liquid helium coolant, and 10 v/o insulation. The magnet shield is taken to be 60 v/o 316 SS, 15 v/o Pb, 15 v/o B_4C and 5 v/o H_2O coolant. The shield has a minimum thickness of .5 m in the quadrupole sections. The inner surface of the shield in the quadrupole section is tapered such that it does not see direct line of sight 14.1 MeV source neutrons. This will be shown to be more advantageous than using a shield with flat inner surface.

The neutronics and photonics calculations are performed using the three-dimensional Monte Carlo code MORSE.[6] A coupled 25 neutron - 21 gamma group cross section library is used. The library consists of the RSIC DLC-41B/VITAMIN-C data library[7] and the DLC-60/MACKLIB-IV response data library.[8] Since only 1/40 of the reactor is considered, we start with 1.775×10^{19} 14.1 MeV fusion neutrons per second and perform target calculations to determine the source intensity and spectrum for neutrons and gammas emitted from the target. These source neutrons and gammas are considered to be emitted isotropically at the origin.

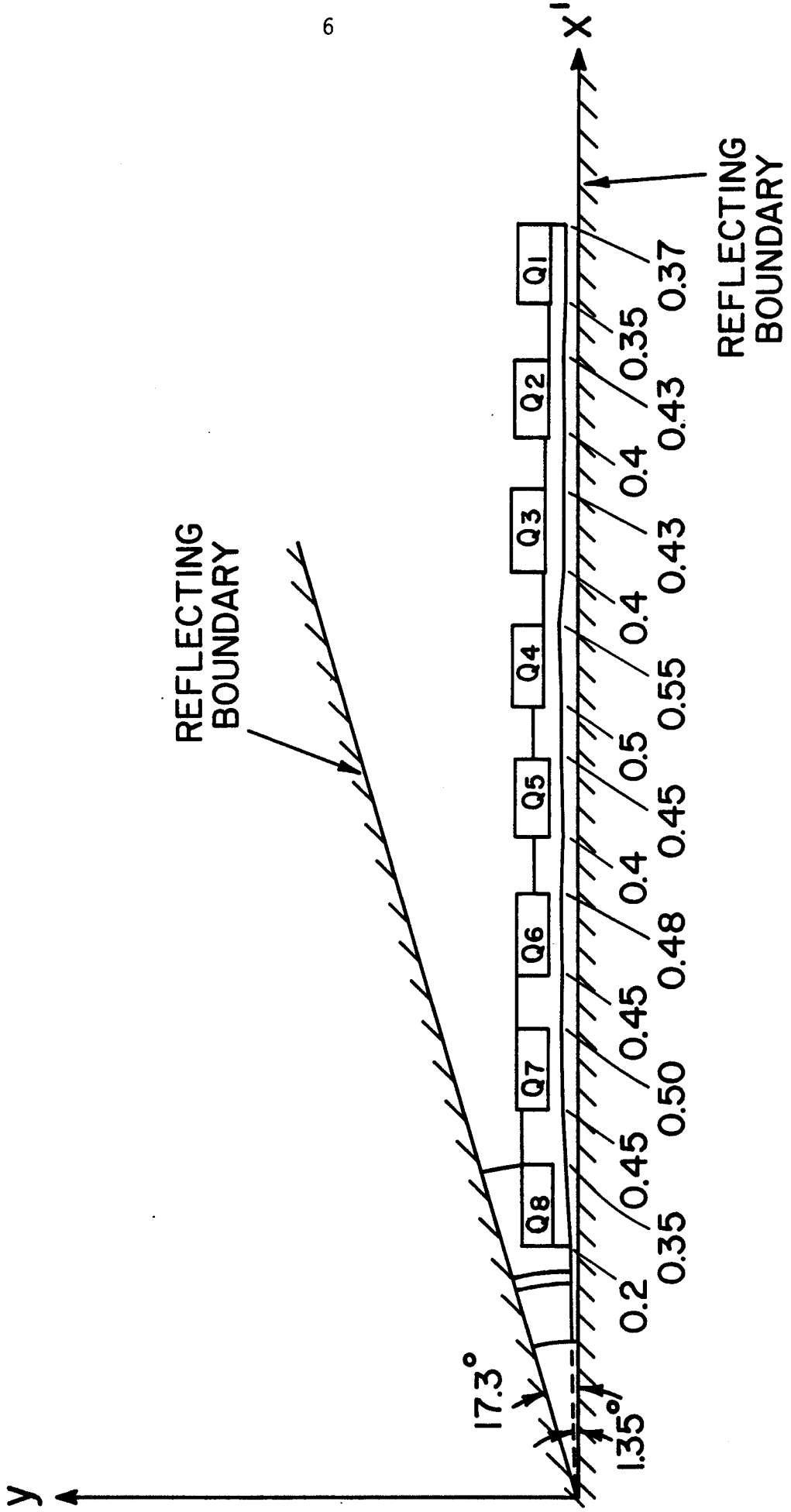

Figure 3 Cross section at plane z'=0 for focussing magnets and shield

In order to get statistically adequate estimates for the flux in the focussing magnets with a reasonable number of histories, an angular source biasing is used. The biasing technique is similar to that used previously for the analysis of the end plug of a tandem mirror fusion reactor.[3] However, in this case, the distribution is biased in both polar and azimuthal angles.

The distribution function from which the polar and azimuthal angles are picked is

$$P(\underline{\Omega})\ d\underline{\Omega} = P(\mu)\ P(\phi)\ d\mu\ d\phi\ . \qquad (1)$$

For the unbiased isotropic distribution we have

$$P(\mu) = 1\ ,\ \mu\varepsilon(0,1)$$

and

$$P(\phi) = 10/\pi\ ,\ \phi\varepsilon(0, \tfrac{\pi}{10})$$

where $\mu=\cos\theta$, and θ and ϕ are the polar and azimuthal angles with respect to the frame xyz. If the biased distribution function is given by

$$P'(\underline{\Omega})d\underline{\Omega} = P'(\mu)\ P'(\phi)\ d\mu\ d\phi\ , \qquad (2)$$

the statistical weight of the source should be modified by the ratio of the unbiased to the biased distribution functions at any particular solid angle (θ,ϕ) for the final estimates to be unbiased. Therefore, the weight for the biased case, w', is related to the weight for the unbiased case, w, by

$$w' = w \frac{P(\mu)P(\phi)}{P'(\mu)P'(\phi)} . \qquad (3)$$

In this work, μ is picked from a biased distribution which forces 90% of the source neutrons to have $\theta_p - \frac{\Delta\theta_p}{2} < \theta < \theta_p + \frac{\Delta\theta_p}{2}$, where $\theta_p = 74^0$ is the angle between the axes x' and z, and $\Delta\theta_p = 8.07^0$ as shown in Fig. 2. A schematic of the biased and unbiased distributions for μ is given in Fig. 4(a). The azimuthal angle, ϕ, is picked from a biased distribution that forces 90% of the source neutrons to have $0 < \phi < \Delta\phi_p$, where $\Delta\phi_p = 1.4^0$ is the azimuthal angle in the plane z=0 subtended by the penetration. A schematic of the biased and unbiased distributions for ϕ is given in Fig. 4(b). After picking μ and ϕ, the direction cosines of the source particle with respect to the frame xyz are calculated. An orthogonal transformation is performed to determine the corresponding direction cosines with respect to the frame x'yz' used in the calculations.

Because of the $1/R^2$ geometrical attenuation, the largest radiation effects occur in the magnets closer to the source. For this reason and to reduce the computing time, only the last two quadrupoles Q_7 and Q_8 are modelled. The geometry for the computational model used in this work is given in Fig. 5. Each quadrupole is divided into three zones and each quadrupole shield is divided into two zones. Zone 12 represents the biological shield. Zones 13 and 14 represent the reflector and blanket, respectively. The inner vacuum region (zone 15) is extended to the region outside the biological shield and the focussing magnets. This allows the neutrons leaking out of the biological shield to have additional collisions in the focussing magnets instead of being discarded as they would be if an outer vacuum region is used. To quantify the leakage through the penetration a 1 cm thick penetration plug is designated as zone 17. The dotted lines in Fig. 5

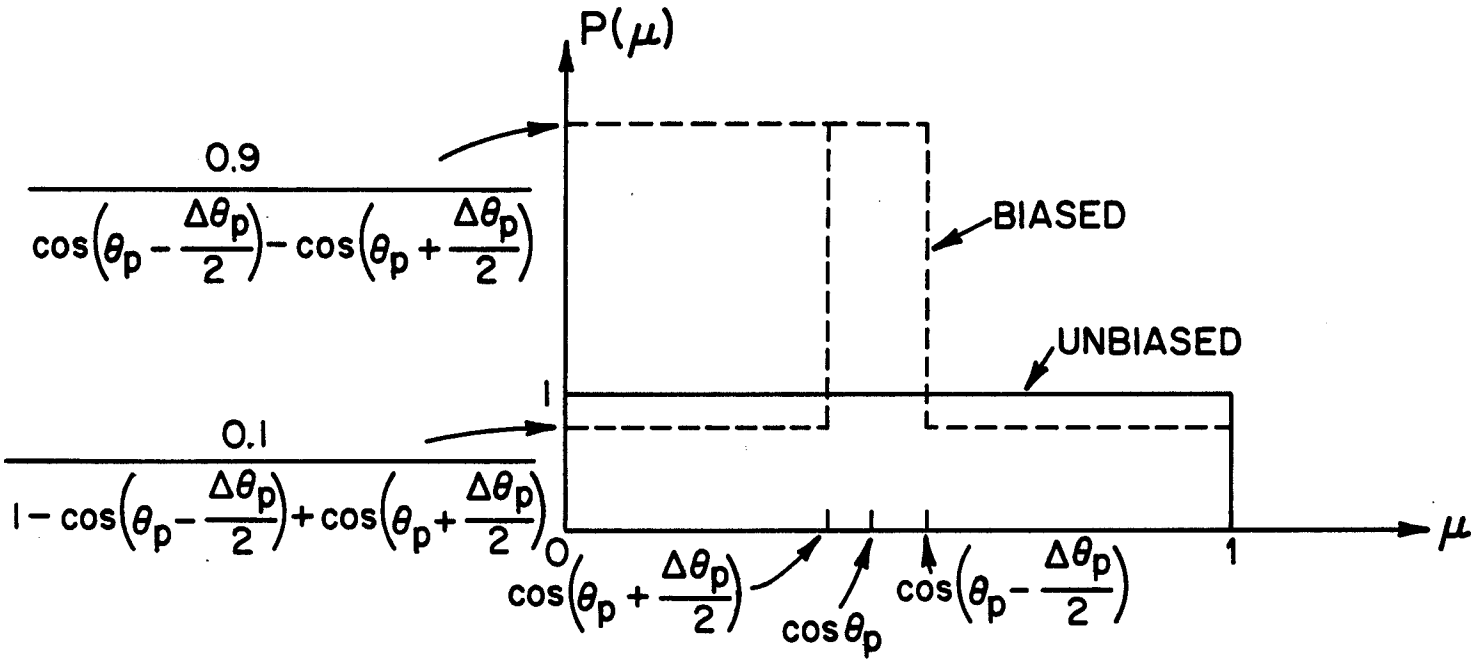

(a) ANGULAR BIASING FOR POLAR ANGLE

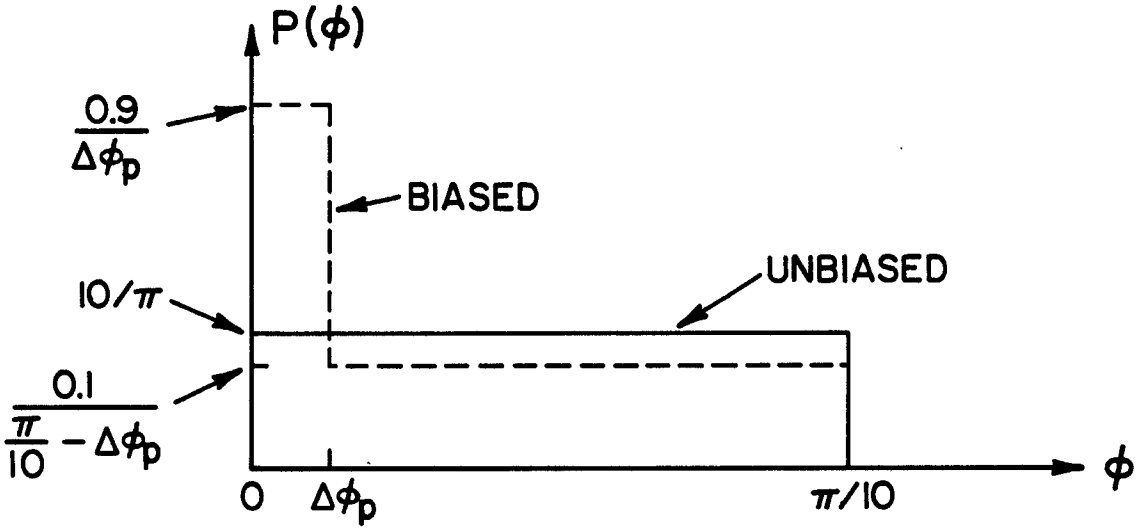

(b) ANGULAR BIASING FOR AZIMUTHAL ANGLE

Figure 4 Angular source biasing scheme

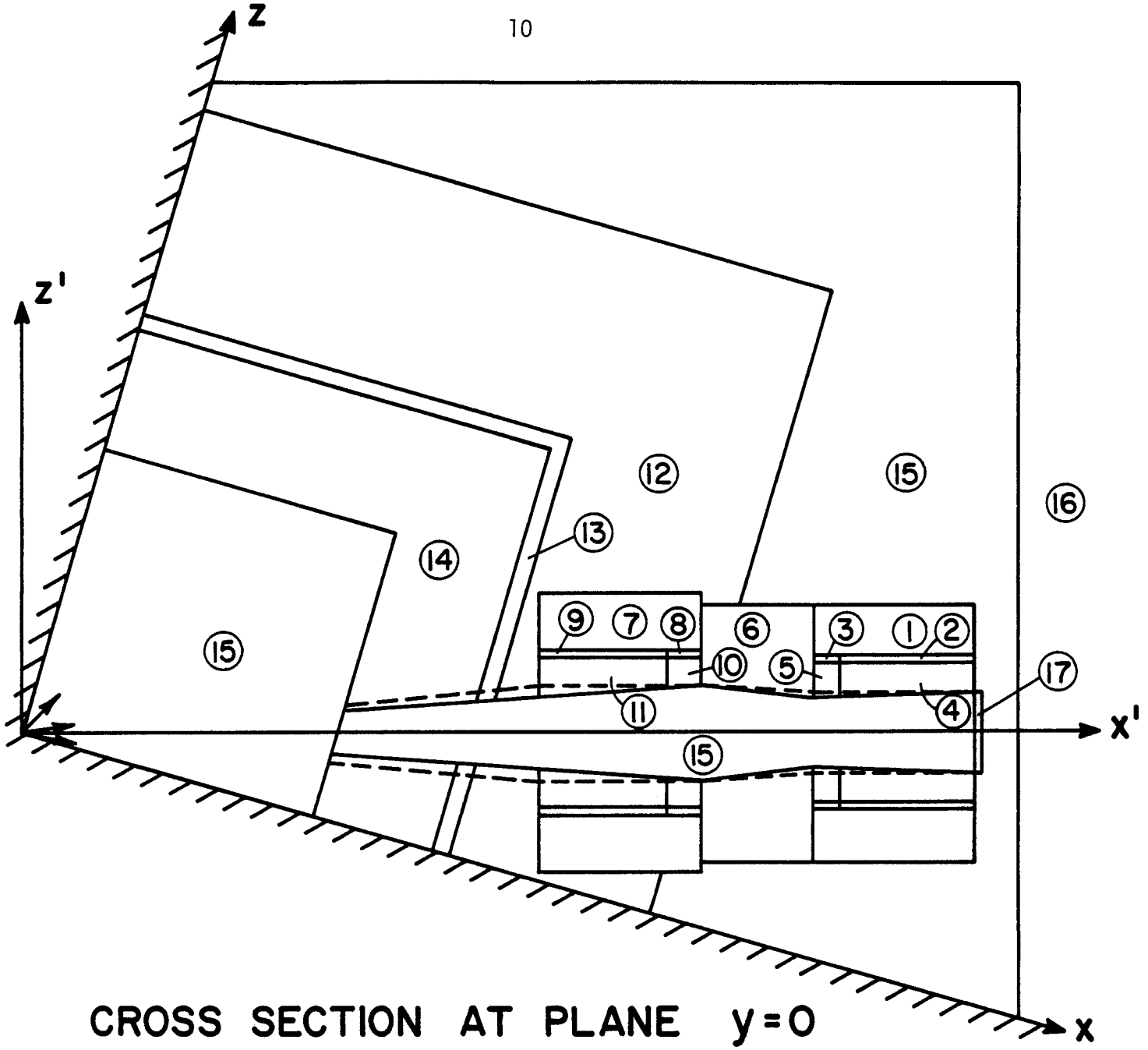

CROSS SECTION AT PLANE y=0

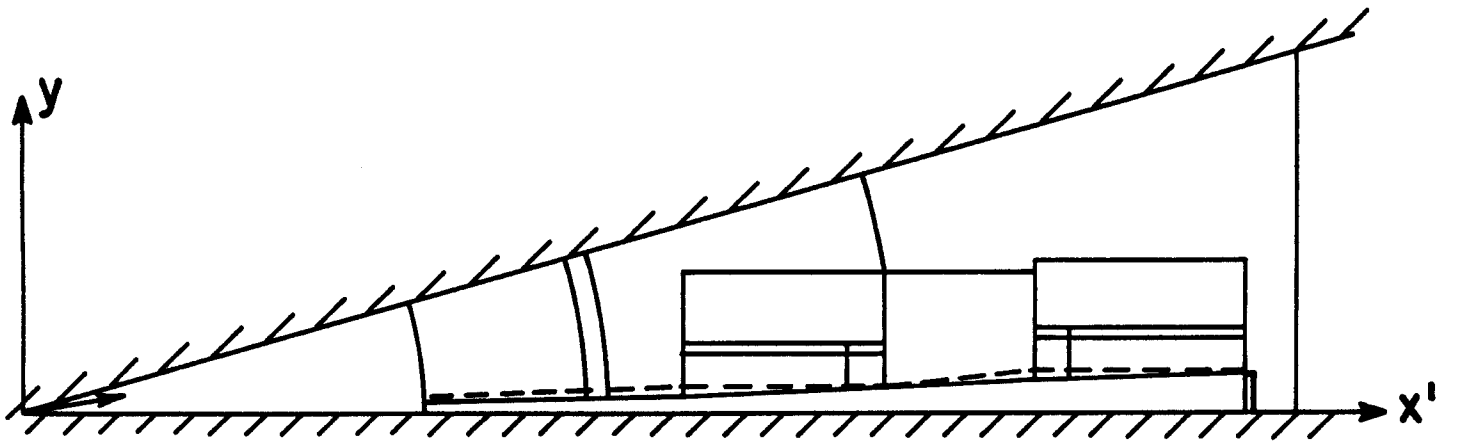

CROSS SECTION AT PLANE z'=0

Figure 5 Geometry of computational model for final two focussing magnets

represent the geometry for a flat shield in the quadrupole sections. The solid lines represent the case with the shield being tapered in the quadrupole sections. Table 1 gives the dimensions and material composition used in the different zones. The results presented are obtained using 20,000 histories in the Monte Carlo problem.

III. Results and Discussion

The effect of tapering the shield in the quadrupole sections on the flux in the magnets was investigated. The geometrical models used for the flat and tapered shield cases are shown in Fig. 5. In the tapered shield case, the shield is tapered along the direct line of sight of source neutrons. In this case, no direct 14.1 MeV source neutrons impinge on the part of the shield in the quadrupole sections. All source neutrons impinge on the inner surface of the shield in the drift section. Table 2 shows the effect of tapering the shield on the neutron scalar flux in the different penetration zones.

It is clear from the results in Table 2 that tapering the shield in the quadrupole sections results in reducing the neutron flux in the magnets. The peak neutron flux in quadrupole 7 occurring in zone 3 is reduced by a factor of 1.8 when the shield is tapered. On the other hand, the peak neutron flux in quadrupole 8 occurring in zone 8 is reduced by an order of magnitude. The effect of shield tapering on the flux in quadrupole 8 is more pronounced than that in quadrupole 7 because scattering of 14.1 MeV neutrons is highly forward peaked. It is clear also that the flux in the shield for quadrupole 8 is reduced significantly by tapering. The reason is that in the tapered case no direct line of sight source neutrons reach zones 10 and 11 and neutrons reach these zones only after having collisions in the drift section shield (zone 6). On the other hand, the neutron flux in the shield for quadrupole 7 decreases only slightly because the 14.1 MeV source neutrons have a larger

Table 1

Zones Used to Model the Final Two Focussing Quadrupoles and Their Shields

Region	Zone Number	Length (m)	Thickness (m) Tapered Shield	Thickness (m) Flat Shield	Material Composition
Quadrupole 7	1	2.7	.9	.9	7.52 v/o NbTi + 67.48 v/o Cu
	2	2.2	.1	.1	+ 15 v/o Liq. He + 10 v/o
	3	.5	.1	.1	Insulation
Shield for Q_7	4	2.2	.5-.55	.5	60 v/o 316 SS + 15 v/o Pb
	5	.5	.54-.56	.5	+ 15 v/o B_4C + 5 v/o H_2O
Drift Section Shield	6	1.8	1.37-1.56	1.35-1.50	
Quadrupole 8	7	2.7	.9	.9	7.52 v/o NbTi + 67.48 v/o Cu
	8	.5	.1	.1	+ 15 v/o Liq. He + 10 v/o
	9	2.2	.1	.1	Insulation
Shield for Q_8	10	.5	.5-.54	.5	60 v/o 316 SS + 15 v/o Pb
	11	2.2	.53-.69	.5	+ 15 v/o B_4C + 5 v/o H_2O
Biological Shield	12	-	3.5	3.5	95 v/o Concrete + 5 v/o H_2O
Reflector	13	-	.4	.4	90 v/o Ferritic Steel + 10 v/o $Li_{17}Pb_{83}$
Blanket	14	-	2.0	2.0	98 v/o $Li_{17}Pb_{83}$ + 2 v/o SiC (.33 d.f.)
Inner Vacuum	15	-	-	-	Void
Outer Vacuum	16	-	-	-	Void
Penetration Plug	17	-	.01	.01	316 SS

Table 2

Effect of Tapering the Shield on the Flux Estimates in Penetration Zones

Region	Zone Number	Neutron Scalar Flux (n/cm^2 s) Flat Shield	Tapered Shield
Quadrupole 7	1	2.767×10^{8} (0.60)*	1.631×10^{8} (0.77)
	2	4.504×10^{9} (0.40)	3.441×10^{9} (0.52)
	3	2.156×10^{10} (0.38)	1.217×10^{10} (0.48)
Shield for Q_7	4	1.552×10^{12} (0.13)	7.728×10^{11} (0.14)
	5	3.606×10^{12} (0.17)	2.224×10^{12} (0.15)
Drift Section Shield	6	1.299×10^{12} (0.09)	9.765×10^{11} (0.08)
Quadrupole 8	7	7.388×10^{9} (0.75)	9.720×10^{6} (0.77)
	8	9.854×10^{10} (0.76)	9.758×10^{9} (0.69)
	9	1.780×10^{11} (0.50)	NS**
Shield for Q_8	10	6.624×10^{12} (0.14)	8.108×10^{11} (0.18)
	11	8.181×10^{12} (0.11)	1.980×10^{11} (0.30)
Penetration Plug	17	5.936×10^{13} (0.13)	5.368×10^{13} (0.10)

* Numbers in parentheses are fractional standard deviations.
** No score in this zone for the 20,000 histories used.

chance to go in the forward direction into zones 4 and 5 than to go in the backward direction into zones 10 and 11 after colliding in the drift section (zone 6). The neutron flux at the first surface of the HIBALL blanket at the reactor midplane is 2.364×10^{14} n/cm^2 s. This implies that the peak flux in the focussing magnets is more than four orders of magnitude lower than the flux at the first surface of the blanket.

The neutron leakage flux at the penetration plug is 5.368×10^{13} n/cm^2 s for the tapered shield case. The direct line of sight 14.1 MeV neutron flux leaking from the penetration is 2.398×10^{13} n/cm^2 s which amounts to 45% of the neutron leakage flux. It is clear from the results in Table 2 that the neutron flux in the penetration plug decreases by tapering the shield. The reason is that the amount of neutrons leaking after colliding along the penetration decreases when no direct line of sight source neutrons are incident on the shield for quadrupole 7. Even though an appreciable amount of neutrons are leaking through the penetration modelled here, this does not pose a serious problem because only the last two quadrupoles are modelled here. The other six quadrupoles are shielded in the same manner as shown in Figs. 2 and 3. Considering $1/R^2$ attenuation, the neutron leakage flux at quadrupole 1 is estimated to be 7.257×10^{12} n/cm^2 s.

Further modification in the shape of the shield in the drift section may be made to improve the effectiveness of the magnet shielding. The inner surface of the shield in the drift section is tapered at both ends such that it coincides with the direct line of sight from the source as shown in Fig. 6. In this case, all source neutrons impinge on a vertical neutron dump in the shield. This results in increasing the minimum distance between the magnet and the point on the surface of the shield where the source neutron has its first collision and is expected to reduce the radiation damage in the

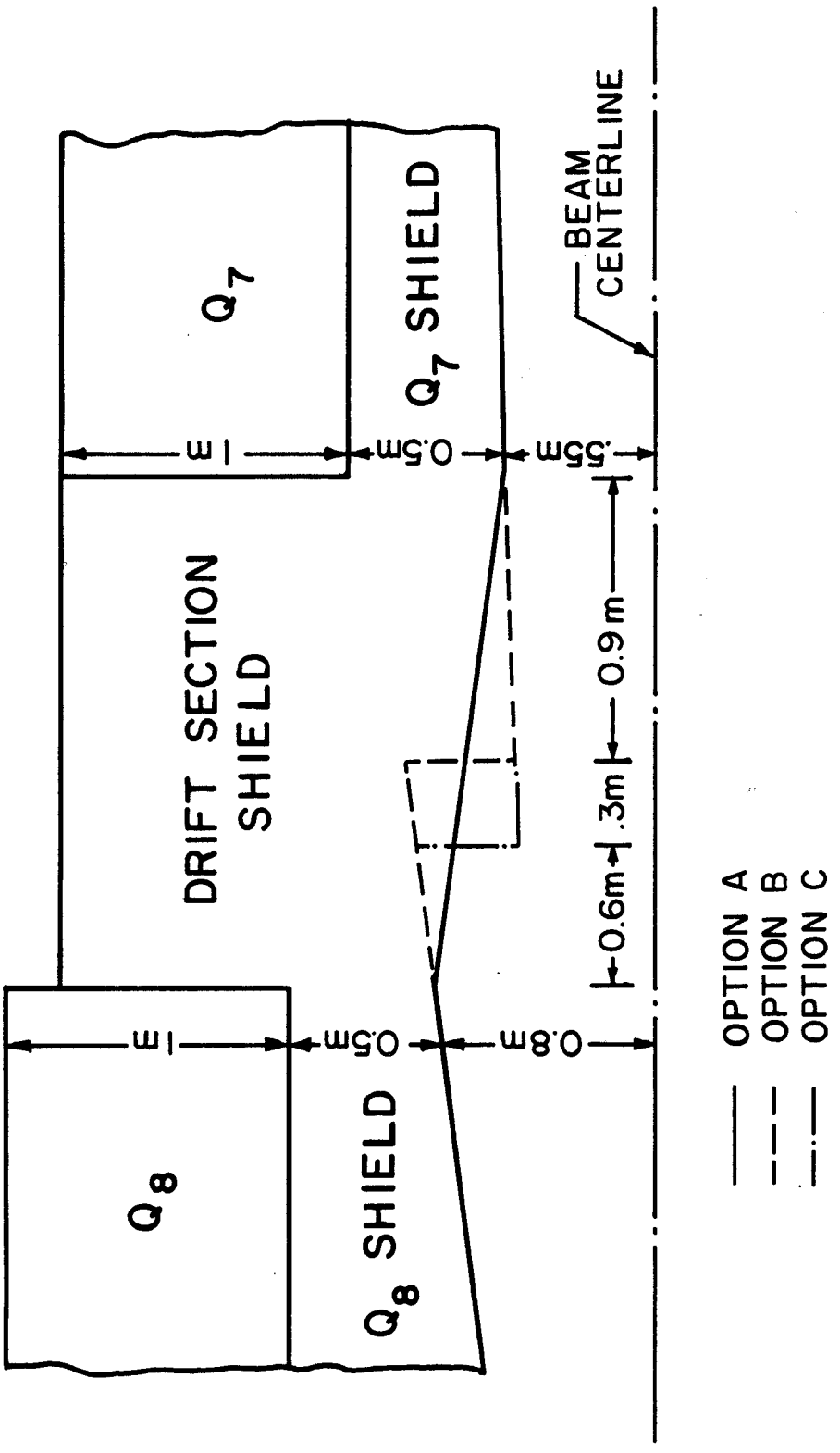

Figure 6 Options for tapering drift section shield

magnets. Two positions are considered for the neutron dump as shown in Fig. 6.

Table 3 gives the atomic displacements per full power year (FPY) in the Cu stabilizer in the different magnet zones for the cases of flat shield and tapered shield with the different options for the drift section shield as shown in Fig. 6. Notice that even though the scalar flux in zones 2 and 3 of quadrupole 7 decreases when the shield is tapered with option A (Table 2), the dpa rate slightly increases. The reason is that when the shield is tapered, all 14.1 MeV source neutrons fall on the drift section shield (zone 6) instead of falling on zones 4 and 5 as well. Since elastic scattering of high energy neutrons is highly forward peaked, this results in a slight increase in the high energy flux in zones 2 and 3 of quadrupole 7 yielding higher dpa values. As the neutrons slow down in the shield the scattering becomes more isotropic with the low energy flux decreasing in zones 2 and 3. The net effect is to decrease the total neutron scalar flux as shown in Table 2. On the other hand, tapering the shield with option A results in significant reduction in the dpa rate in quadrupole 8.

If shielding option B is used, it is found that the peak dpa rate in quadrupole 7 is decreased by a factor of ~ 6 as compared to option A in addition to decreasing the peak dpa rate in quadrupole 8 significantly. In the run of 20,000 histories, no contribution was obtained in quadrupole 8. Because scattering is forward peaked at high neutron energies, locating the source neutron dump halfway between Q_7 and Q_8 results in considerable reduction in damage in Q_8 and a smaller reduction in Q_7. Using option A the peak damage occurs in Q_8 while it occurs in Q_7 when option B is used. In option C, the source neutron dump is moved closer to Q_8. This is found to decrease the peak dpa rate in Q_7 considerably and increase the peak damage

Table 3

Effect of Penetration Shield Shape
on DPA Rate in the Copper Stabilizer

Region	Zone Number	DPA Rate (dpa/FPY) Flat Shield	Tapered Shield in Quadrupole Section Option A	Option B	Option C
Quadrupole 7	1	2.167×10^{-6}	1.142×10^{-6}	1.023×10^{-7}	NS
	2	3.129×10^{-5}	3.686×10^{-5}	1.256×10^{-5}	NS
	3	9.115×10^{-5}	9.702×10^{-5}	1.600×10^{-5}	2.710×10^{-6}
Quadrupole 8	7	1.690×10^{-5}	1.742×10^{-7}	NS	1.749×10^{-8}
	8	6.182×10^{-4}	1.151×10^{-4}	NS	4.483×10^{-6}
	9	1.056×10^{-3}	NS	NS	7.580×10^{-7}

rate in Q_8 only slightly. The peak in Q_8 when option C is used is a factor of ~ 25 lower than that when option A is used.

Table 4 gives the radiation dose rate in the epoxy electrical insulation in the different magnet zones for the different geometrical options considered. Again, it is clear that significant reduction in the radiation dose is obtained when the suggested shield geometrical modifications are adopted. The results given in Table 4 include the contribution from both neutron and gamma energy deposition. Table 5 gives the peak dpa rate, the peak radiation dose, and the peak power density in the focussing magnets for the different geometrical options considered. It is clear that the tapered shield with option C is the most effective shield design. Using option C for the drift section shield is found to result in a peak dpa rate in the Cu stabilizer of only 4.483×10^{-6} dpa/FPY. The neutron leakage flux at the penetration plug is found also to decrease to a value of 4.615×10^{13} n/cm^2 s with option B and 3.361×10^{13} n/cm^2 s for option C. This results from increasing the attenuation distance in the shield for neutrons impinging on the source neutron dump.

Radiation damage to the stabilizing material in the superconducting magnets results in increasing the electrical resistivity. The radiation induced resistivity is related to the number of displacements per atom in the stabilizer. A 50% radiation induced resistivity increase in the copper stabilizer was used as the design criterion. A resistivity increase of this amount is produced by a damage level of 1.4×10^{-4} dpa. This value is obtained using the relation between the induced resistivity in Cu, ρ_i, and the total displacements per atom, d, given by the following equation[9]:

$$\rho_i = 3 \times 10^{-7} \left(1 - e^{-563d}\right) \Omega \cdot \text{cm} . \qquad (4)$$

Table 4

Effect of Penetration Shield Shape on Radiation Dose Rate in the Epoxy Insulation

Region	Zone Number	Radiation Dose Rate (Rad/FPY) Flat Shield	Tapered Shield in Quadrupole Section Option A	Option B	Option C
Quadrupole 7	1	5.220×10^{6}	2.149×10^{6}	7.966×10^{5}	1.625×10^{2}
	2	5.914×10^{7}	7.637×10^{7}	1.978×10^{7}	7.390×10^{3}
	3	1.831×10^{8}	2.195×10^{8}	2.526×10^{7}	4.174×10^{6}
Quadrupole 8	7	4.961×10^{7}	3.350×10^{5}	NS	1.031×10^{5}
	8	1.616×10^{9}	2.552×10^{8}	NS	7.188×10^{6}
	9	3.467×10^{9}	NS	NS	1.250×10^{6}

Table 5

Effect of Penetration Shield Shape on Peak Values of DPA, Radiation Dose, and Nuclear Heating in the Focussing Magnets

	Flat Shield	Tapered Shield in Quadrupole Section Option A	Option B	Option C
Peak dpa/FPY in Cu Stabilizer	1.056×10^{-3}	1.151×10^{-4}	1.600×10^{-5}	4.480×10^{-6}
Peak Radiation Dose in Insulation	3.467×10^{9}	2.552×10^{8}	2.526×10^{7}	7.20×10^{6}
Peak Power Density (W/cm^3)	4.380×10^{-3}	2.44×10^{-4}	3.554×10^{-6}	5.350×10^{-7}

However, complete recovery is possible by annealing. Increasing the time span between required anneals is desirable for reducing maintenance costs. Decreasing the number of anneals required during the reactor lifetime also minimizes any possible undesirable consequences of cyclic irradiation. Using the shield design with option C, the maximum period of operation without annealing is ~ 31 full power years. This is compared to 8.5 FPY when option B is used and ~ 1 FPY when option A is used. If a flat shield design is used, one needs to anneal every ~ 45 days. This implies that when the shield design with option C is used, no annealing is needed for an estimated reactor lifetime of 20 full power years.

The radiation effects on the insulator are not reversible and it is essential that it lasts the whole reactor lifetime. The design limit used for the radiation dose in the epoxy electrical insulator is 5×10^9 rad. The results show that for an estimated reactor lifetime of 20 full power years, the designs with options B and C result in an accumulated radiation dose well below the design limit, while the designs with a flat shield and with option A do not satisfy the design criterion. The design limit on the peak power density is set to be 10^{-4} W/cm^3. It is clear from the results of Table 5 that the tapered shield design with options B and C satisfy this design criterion while the designs with a flat shield and option A do not fulfill this requirement. It is concluded from the results presented here that a magnet shield which is tapered in the quadrupole sections with option C for the drift section shield shape satisfies the design criteria on the radiation dose in the insulator and the nuclear heating in the magnet with the possibility of eliminating the need for magnet annealing during the whole reactor lifetime.

IV. Summary and Conclusions

A three-dimensional neutronics and photonics analysis was performed for the heavy ion beam line penetration in the HIBALL fusion reactor. Various penetration shield geometrical options were considered to assess their effectiveness in reducing the radiation effects in the beam focussing magnets. Tapering the shield in the quadrupole sections in such a way that all direct line of sight 14.1 MeV source neutrons fall on the inner surface of the drift section shield was found to reduce the radiation damage in the magnets. Several options for the shape of the shield in the drift sections were analyzed. The smallest radiation effects in the magnet were obtained when the inner surface of the shield in the drift sections is also tapered resulting in a vertical neutron dump between the magnets. Better shielding was obtained with the neutron dump between the last two quadrupoles placed closer to the last quadrupole. With this design, the period between required magnet anneals was increased to ~ 31 full power years compared to 45 days for the flat shield design. This implies that using the recommended shield design, the need for annealing during the reactor lifetime can be eliminated completely. The shield design recommended reduces the peak radiation dose in the insulator allowing it to last for the whole reactor lifetime. The peak power density in the magnet is also reduced significantly.

Acknowledgement

Support for this work was provided by the Kernforschungszentrum Karlsruhe and the Bundesministerium für Forschung und Technologie, Federal Republic of Germany, under research agreement with Fusion Power Associates, Gaithersburg, MD.

References

1. J. Jung and M.A. Abdou, Nuclear Technology, 41, 71 (1978).

2. M. Ragheb, A. Klein, and C.W. Maynard, Nuclear Technology/Fusion, 1, 99 (1981).

3. M. Ragheb and C.W. Maynard, UWFDM-398, University of Wisconsin (1981).

4. M. Sawan, W. Vogelsang, and G. Moses, UWFDM-395, University of Wisconsin (1980).

5. RSIC Code Package CCC-254, "ANISN-ORNL", Radiation Shielding Information Center, ORNL.

6. RSIC Code Package CCC-203, "MORSE-CG", Radiation Shielding Information Center, ORNL.

7. RSIC Data Library Collection, "VITAMIN-C, 171 Neutron, 36 Gamma-Ray Group Cross Sections Library in AMPX Interface Format for Fusion Neutronics Studies", DLC-41, ORNL.

8. RSIC Data Library Collection, "MACKLIB-IV, 171 Neutron, 36 Gamma-Ray Group Kerma Factor Library", DLC-60, ORNL.

9. M. Abdou, J. Nucl. Matls. 72 147 (1978).